Modeling the decoupling of the hemodynamic and metabolic responses to neural stimulus in the primary visual cortex

Aaron Simon
BENG 260
Neruodynamics Final Project

Abstract

Stimulus-evoked neural activity increases both local oxygen metabolism and blood flow in active regions of the brain. However, multiple imaging modalities including functional magnetic resonance imaging and positron emission tomography have demonstrated that the degree of coupling between metabolism and blood flow is highly non-linear. Specifically oxygen metabolism appears to peak and decline at significantly lower levels of stimulus than does blood flow. This model attempts to explain this phenomenon as a consequence of balanced excitation and inhibition in a network of neurons in the primary visual cortex.

1 Introduction

Since the 1990 discovery of the blood oxygenation level dependent (BOLD) signal, functional magnetic resonance imaging (fMRI) has been used extensively to study neural activity in the brain[1]. However, as the BOLD signal is modulated both by neuronal metabolism and cerebral blood flow (CBF), quantitating neural activity based on functional imaging requires a precise understanding of the coupling between these two processes. An often-observed phenomenon in functional studies including positron emission tomography (PET) and functional magnetic resonance imaging (fMRI) is that the coupling of oxygen metabolism and blood flow in the brain is highly non-linear [2]. Specifically, with increases in stimulus frequency or contrast, the cerebral metabolic rate of oxygen ($CMRO_2$) appears to saturate at a lower value than does CBF, causing the coupling ratio $n = \frac{\Delta CBF}{\Delta CMRO_2}$ to increase with increasing frequency or contrast [2]. The physiology underlying this observed decoupling of CBF and CMRO2 is incompletely understood, however, recent studies of neurovascular coupling have generated several theories. One predominant theory is that the activity-driven increase in CBF, termed functional hyperemia, is not tied directly to the increased metabolic demands of active neurons, but instead driven by the release of vasoactive molecules from either glial cells or from the neurons themselves [3]. Several potential mediators of functional hyperemia have been identified, including nitric oxide (NO) released from GABA-ergic interneurons [4] and prostaglandins released from glutamate-sensitive astrocytes [5].

While it is likely that in a given region of cortical tissue, several cellular and molecular mediators participate in the hemodynamic response, neural networks in all regions of the brain that demonstrate neurovascular decoupling must be arranged in such a way that the stimulus-threshold for the saturation of hemodynamic activity exceeds the threshold for the saturation of metabolic activity. The separation of these stimulus thresholds may be accomplished in several ways. For example, in the rat barrel cortex, Devor *et al* found that the hemodynamic response within a given barrel was a function of the electrophysiological activity occurring over a much broader spatial domain. Accordingly, they found that while neural activity within the principle barrel saturated rapidly in response to whisker-deflection, the blood flow to the barrel increased throughout the stimulus range due to continuously increasing neural activity in neighboring barrels [6]. The purpose of this model is to

explore the possibility that neurovascular decoupling can arise from a single cortical column as a consequence of the balance between excitatory and inhibitory neurons within the column. Other cortical models have demonstrated that balanced excitation and inhibition can produce highly variable spiking in response to an invariant stimulus [7]. This model seeks to determine whether balanced excitation and inhibition can produce variability in the spike frequencies of sub-populations of neurons within a single column. It then attempts to demonstrate how the active release of vasoactive molecules from one of these sub-populations or from the astrocytes with which the neurons interact can produce the nueral-vascular decoupling observed in functional imaging studies.

2 Methods

2.1 Neuron biophysics and network architecture

The neurons in this system are modeled as described by Hodgkin and Huxley [8] such that the membrane potential of each neuron in isolation may be described by

$$C\frac{dV}{dt} = (-g_K n^4(V - E_K) - g_{Na} m^3 h(V_i - E_{Na}) - g_L(V - E_L)) \tag{1}$$

where each current represents a potassium, sodium, or leak channel, respectively and

$$\begin{aligned}
\frac{dn}{dt} &= \alpha_n(1-n) - \beta_n n && (2)\\
\frac{dm}{dt} &= \alpha_m(1-m) - \beta_m m && (3)\\
\frac{dh}{dt} &= \alpha_h(1-h) - \beta_h h && (4)\\
\alpha_m(V) &= 0.1\ (V+40)/(1-\exp(-(V+40)/10)) && (5)\\
\beta_m(V) &= 4\ \exp(-(V+65)/18) && (6)\\
\alpha_h(V) &= 0.07\ \exp(-(V+65)/20) && (7)\\
\beta_h(V) &= 1/(1+\exp(-(V+35)/10)) && (8)\\
\alpha_n(V) &= 0.01\ (V+55)/(1-\exp(-(V+55)/10)) && (9)\\
\beta_n(V) &= 0.125\ \exp(-(V+65)/80) && (10)
\end{aligned}$$

describe the gating of the ion channels. The values of all constant parameters are listed in table 1. in addition, the voltage of each neuron may be modulated by an inhibitory GABA synapse and as many as three excitatory glutamate synapses whose effects on the membrane potential of a post-synaptic neuron may be described by

$$C\frac{dV_{post}}{dt} = g_j r_j (V_{post} - E_j) \tag{11}$$

where the gating of the ligand gated channel is described by

$$\frac{dr_j}{dt} = \alpha_{rj} \cdot T_r(V_{pre}) \cdot (1 - r_j) - \beta_{rj} r \tag{12}$$

and the available neurotransmitter in the synapse is a function of the voltage of the pre-synaptic neuron V_{pre}, and is described by

$$T_r(V_{pre}) = \frac{T_{max}}{1 + \exp(-\frac{V_{pre} - V_p}{K_p})} \tag{13}$$

An additional current I_{inj} will be injected into a single neuron located in the thalamus to represent an incoming stimulus. The magnitude of this current will be varied from $10 - 50 \frac{\mu A}{cm^2}$ to simulate stimuli of varying strength. The architecture of the of the neural network is based on the LAMINART model of the primary visual cortex (V1) because of its simplicity, balance of excitatory and inhibitory neurons, and single thalamic input [9]. Some further modifications were made to simplify the effects of top-down inputs from secondary visual cortex V2 and from neighboring cortical columns. Briefly, these modifications consisted of reducing input from V2 to a simple positive-feedback loop with

Table 1: Model Parameters

Parameter	Value	Parameter	Value
C	$1\frac{\mu F}{cm^2}$	K_p	$5mV$
g_{Na}	$120\frac{mS}{cm^2}$	V_p	$7mV$
g_K	$36\frac{mS}{cm^2}$	g_{glu}	$0.01\frac{mS}{cm^2}$
g_L	$0.3\frac{mS}{cm^2}$	E_{glu}	$-33mV$
E_{Na}	$50mV$	α_{glu}	$2.4mM^{-1}ms^{-1}$
E_K	$-77mV$	β_{glu}	$0.56ms^{-1}$
E_L	$-54.387mV$	$Tmax_{glu}$	$1.0mM$
g_{GABA}	$3\frac{mS}{cm^2}$	α_{sGC}	$1.667mM^{-1}ms^{-1}$
E_{GABA}	$-75mV$	β_{sGC}	$0.0037ms^{-1}$
α_{GABA}	$5mM^{-1}ms^{-1}$	$Tmax_{NO}$	$0.02mM$
β_{GABA}	$0.1 - 0.2ms^{-1}$	α_{mGluR}	$0.0067mM^{-1}ms^{-1}$
$Tmax_{GABA}$	$1.5mM$	β_{mGluR}	$8.7 \times 10^{-4}ms^{-1}$

the layer 2 neuron in V1 and reducing input from horizontal layer 2/3 connections to balanced positive/negative-feedback loops with the layer 2 and 3 neurons in V1 (figure 1). The effects of more completely describing top-down and horizontal input on neurovascular decoupling will be explored in a future model.

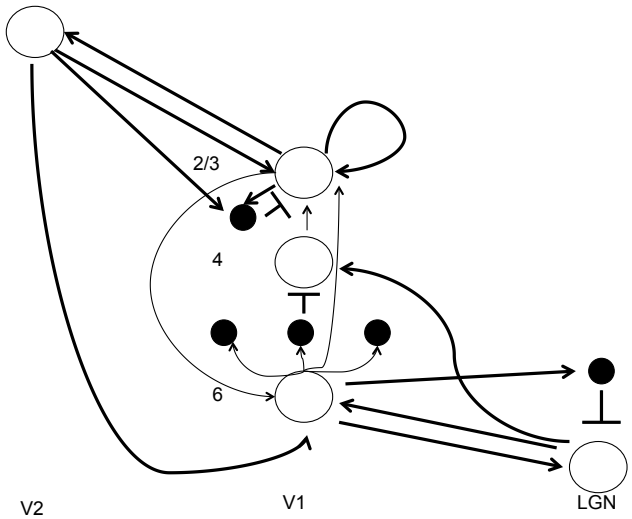

Figure 1: Modified LAMINART model of lateral geniculate nucleus of the thalamus (LGN), V1, and V2. Excitatory neurons are white, inhibitory neurons are black. Numbers in V1 column refer to cortical layer.

2.2 Modeling metabolic activity

The metabolic cost of neural activity will be modeled based on the findings of Attwell and Laughlin who found that the metabolic costs of action potentials and glutamate signaling (including pre-synaptic Ca^{2+} entry, post-synaptic currents, and recycling) to account for the vast majority of the metabolic cost of neural activity and to require approximately $3.84 \times 10^8 ATP$ and $3.28 \times 10^8 ATP$, respectively, per event [10]. As such, in this model, each action potential that occurs in V1 will be assigned a cost of $3.84 \times 10^8 ATP$ and each glutamatergic signaling event will be assigned a cost of $3.28 \times 10^8 ATP$.

2.3 Modeling the hemodynamic response

In this paper two potential mechanisms for the hemodynamic response to neural activity were considered. First, based on the findings of Rancillac et al. [4], it was assumed that inhibitory interneurons containing GABA and NO mediated the hemodynamic response. The release of NO was assumed to be proportional to the spike frequency of the interneurons, i.e. that a quantum of NO was released into the synaptic space with every interneuron action potential. The NO was then allowed to diffuse away from the synaptic space with a diffusion coefficient $D_{NO} = 3.3\frac{\mu m^2}{ms}$ [11]. *In vivo* NO mediates vasodilation through interaction with soluble guanylyl cyclase (sGC) in the smooth muscle cells of muscular arterioles [12]. Guanylyl cyclase produces cyclic guanosine monophosphate (cGMP) which causes relaxation of vascular smooth muscle cells via several pathways including cyclic nucleodtide-gated ion channels [13] and protein kinase G [14]. Here, because the kinetics of NO diffusion and cGMP production are significantly slower than those of neural activity, vasodilation was measured by the production of cGMP, the kinetics of which were modeled by the equation

$$\frac{d[cGMP]}{dt} = \alpha_{sGC}[NO] - \beta_{sGC}[cGMP] \tag{14}$$

As the true distance between the vascular smooth muscle and synaptic space was unknown, production of cGMP was measured at 1,5, and $10\mu m$. To determine whether neurovascular decoupling was sensitive to choice of interneuron sub-population, models in which all interneurons or only layer 5 interneurons mediated the hemodynamic response were considered. Second, it was considered whether a glutamate-sensitive astrocyte could mediate neurovascular decoupling in this model. *In vivo* astrocyte processes are in intimate contact with both synapses and vascular smooth muscle cells [3]. Astrocytes express metabotropic glutamate receptors (mGluR), which are G-protein coupled receptors with many down-stream molecular targets. Among these is the cyclo-oxygenase enzyme, which produces a class of vasoactive molecules called prostaglandins in response to glutamate release from excitatory neurons [15]. Petzold et al. have demonstrated that in rat olfactory-bulb functional hyperemia is mediated primarily through astrocytes via mGluR5 [5]. To simulate this here a model astrocyte was constructed. This astrocyte consisted of metabotropic glutamate receptors in intimate contact with each glutamatergic synapse in V1. The hemodynamic activity at any given time was modeled as the instantaneous sum of the activity of all of the astrocyte's mGlu receptors. Although the kinetics of G-protein coupled receptors are complex [16] they were modeled here to the equation

$$\frac{d(mGluR)}{dt} = \alpha_{mGluR} \cdot T_{glu}(V_{pre}) \cdot (1 - mGluR) - \beta_{mGluR} mGluR \tag{15}$$

with the on and off rates $\alpha_{mGluR} = 0.0067 mM^{-1} ms^{-1}$ and $\beta_{mGluR} = 8.7 \times 10^{-4} ms^{-1}$ based on the kinetics of other G protein-coupled receptors [16].

3 Results

3.1 Linear increases in stimulus current produce variable spike rates across neural network

Changes in spike rate in response to linear increases in thalamic input current were found to be highly variable across the neural network (figure 2). While the thalamic and layer 5 interneurons responded to increased input with monotonic increases in spike rate, the layer 2 and layer 4 excitatory neurons and the layer 3 inhibitory neuron reached peak spike frequency at $30\frac{\mu A}{cm^2}$ input current.

3.2 Variance in spike-rate response to increased stimulus leads to decoupling of metabolic and hemodynamic activity in NO-based model

Increasing injected current linearly from $10 - 50\frac{\mu A}{cm^2}$ caused metabolic activity to peak at $30\frac{\mu A}{cm^2}$ injected current (figure 3a). The subsequent decrease in metabolic activity was driven largely by the decrease in spiking in the layer 2 and layer 4 excitatory neurons above this threshold. Conversely, hemodynamic activity continued to increase throughout the tested range of stimulus amplitudes, as measured by the production of cGMP, regardless of diffusion distance (figure 3b). The continued

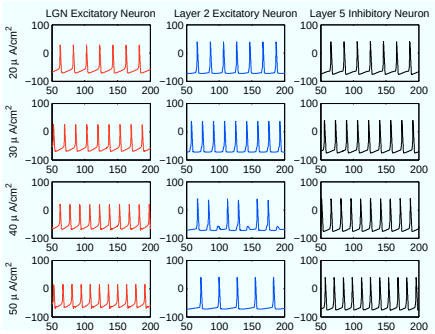

Figure 2: Representative selection of neural response to increased thalamic input. Thalamic neuron (red) and layer 5 interneuron (black) spike rate increased monotonically in response to increased stimulus while layer 2 excitatory neuron (blue) reaches maximum spike rate at $30\frac{\mu A}{cm^2}$. Time measured in milliseconds.

increase in cGMP production was driven by the monotonic increase in spike rate of layer 5 interneurons throughout the stimulus range. As such, decoupling was most pronounced in the model in which NO release was restricted to this sub-population of interneurons (figure 3c). Decoupling was attenuated, though still present, in the model in which all interneurons released NO, due to a decrease in the rate of spiking of the layer 3 interneuron above the threshold of $30\frac{\mu A}{cm^2}$. Decoupling was also sensitive in this model to alterations of the kinetics of inhibitory synapses. Decreasing the duration of inhibitory signals by increasing β_{GABA} from $0.1 - 0.2ms^{-1}$ completely abolished neurovascular decoupling in this model because, under this condition, inhibitory neurons maintained the same spike frequency as excitatory neurons throughout the stimulus range (data not shown).

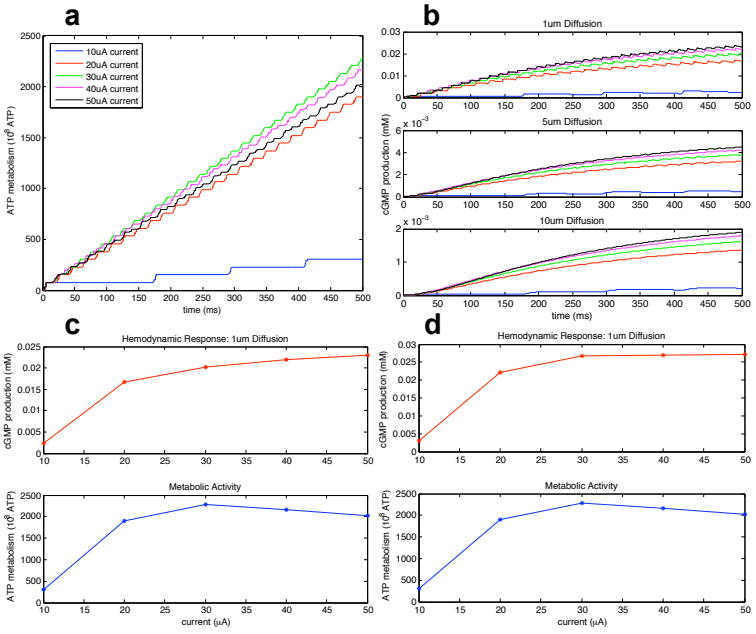

Figure 3: Nitric Oxide model produces neurovascular decoupling for input current $I_{inj} > 30\frac{\mu A}{cm^2}$.a) Metabolic activity due to action potentials and glutamate signaling reaches a maximum at $I_{inj} = 30\frac{\mu A}{cm^2}$. b) cGMP production continues to increase throughout range of stimuli regardless of diffusion distance. Decoupling of hemodynamic and metabolic response was more pronounced when NO release was restricted to layer 5 interneurons (c) than to all interneurons (d)

3.3 Astrocyte model of functional hyperemia does not produce neurovascular decoupling

Unlike the NO-based model, the model in which a glutamate-sensitive astrocyte mediated the hemodynamic response did not produce nueral-vascular decoupling. Instead, both metabolic and hemodynamic activity (as measured by mGluR activity) reached their peak values at $I_{inj} = 30\frac{\mu A}{cm^2}$ and declined for higher levels of input current (figure 4). This is most likely because glutamate release in this model is a principle driver of both hemodynamic and metabolic activity. Becuase the astrocyte model determines hemodynamic activity based on the release of glutamate rather than the spiking of the excitatory neurons, and because the axon terminals of each excitatory neuron in this model are distributed across several cortical layers (figure 1), it was decided not to attempt to restrict control over the hemodynamic response to any smaller sub-population of neurons, as was done with the NO model.

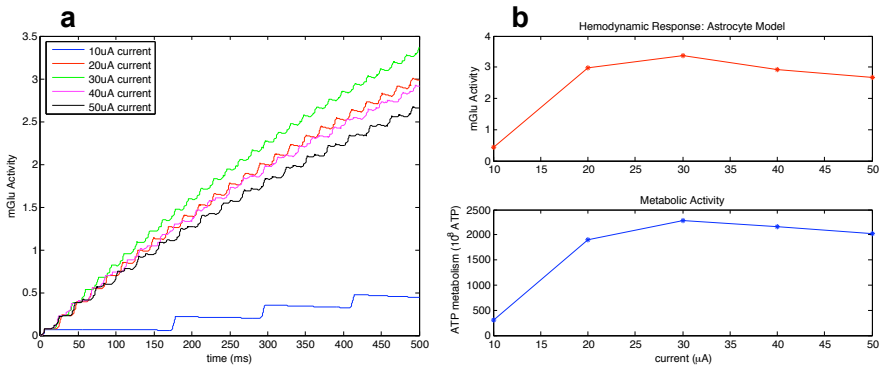

Figure 4: Astrocyte model does not produce neurovascular decoupling. a) Hemodynamic activity as measured by mGluR activity reaches a peak at $I_{inj} = 30\frac{\mu A}{cm^2}$. b) Both metabolic and hemodynamic activity decline for $I_{inj} > 30\frac{\mu A}{cm^2}$.

4 Disussion and Future Work

This model demonstrates that decoupling of the metabolic and hemodynamic responses to neural stimulus may arise in a single cortical column under certain conditions. Specifically this model produced decoupling under the assumptions that the hemodynamic response was mediated by NO-producing inhibitory neurons and that inhibitory signals have a low off-rate, β_{GABA}. The observed decoupling appeared to occur as a consequence of the balance between excitatory and inhibitory neurons in the model. As increasing the input current increased the spiking of both excitatory and inhibitory neurons, certain neurons began to spike at a lower rate than the thalamic input, while others continued in spike at higher frequencies. As the layer 5 interneurons were amongst this latter group, NO release and cGMP production continued to increase even as overall metabolic activity declined. The sensitivity of the model to the value to the parameter β_{GABA} suggests that this decoupling phenomenon was highly sensitive to the balance of excitatory and inhibitory activity in the neural network. That this model failed to produce decoupling under the assumption that glutamate-sensitive astrocytes mediate the hemodynamic response should by no means be taken as evidence against the astrocyte model of functional hyperemia. However, it does raise an intriguing question. By what means can a system in which glutamate signaling drives both metabolic and hemodynamic activity produce this decoupling phenomenon? One possibility is that hemodynamic response is not just a function of intra-columnar activity, but of neural activity occurring over a much wider spatial domain [6]. This would allow surrounding columns receiving sub-threshold inputs to continue to increase blood flow to a column that has received a supra-threshold stimulus. In the future this question may be examined by constructing networks of parallel columns that communicate via synapses in layers 2 and 3. Other areas to be explored by future models include the effects of non-constant input currents, the effects of temporal delays in inter-neuronal communication, and the effects of noise on both the dynamics of neuron spiking and on neurovascular coupling.

References

[1] S. Ogawa, T. M. Lee, A. R. Kay, and D. W. Tank. Brain magnetic resonance imaging with contrast dependent on blood oxygenation. *Proc. Natl. Acad. Sci. U.S.A.*, 87:9868–9872, Dec 1990.

[2] A. L. Lin, P. T. Fox, Y. Yang, H. Lu, L. H. Tan, and J. H. Gao. Evaluation of MRI models in the measurement of CMRO2 and its relationship with CBF. *Magn Reson Med*, 60:380–389, Aug 2008.

[3] C. Iadecola. Neurovascular regulation in the normal brain and in Alzheimer's disease. *Nat. Rev. Neurosci.*, 5:347–360, May 2004.

[4] A. Rancillac, J. Rossier, M. Guille, X. K. Tong, H. Geoffroy, C. Amatore, S. Arbault, E. Hamel, and B. Cauli. Glutamatergic Control of Microvascular Tone by Distinct GABA Neurons in the Cerebellum. *J. Neurosci.*, 26:6997–7006, Jun 2006.

[5] G. C. Petzold, D. F. Albeanu, T. F. Sato, and V. N. Murthy. Coupling of neural activity to blood flow in olfactory glomeruli is mediated by astrocytic pathways. *Neuron*, 58:897–910, Jun 2008.

[6] A. Devor, I. Ulbert, A. K. Dunn, S. N. Narayanan, S. R. Jones, M. L. Andermann, D. A. Boas, and A. M. Dale. Coupling of the cortical hemodynamic response to cortical and thalamic neuronal activity. *Proc. Natl. Acad. Sci. U.S.A.*, 102:3822–3827, Mar 2005.

[7] M. N. Shadlen and W. T. Newsome. The variable discharge of cortical neurons: implications for connectivity, computation, and information coding. *J. Neurosci.*, 18:3870–3896, May 1998.

[8] A. L. HODGKIN and A. F. HUXLEY. A quantitative description of membrane current and its application to conduction and excitation in nerve. *J. Physiol. (Lond.)*, 117:500–544, Aug 1952.

[9] S. Grossberg. How does the cerebral cortex work? Development, learning, attention, and 3-D vision by laminar circuits of visual cortex. *Behav Cogn Neurosci Rev*, 2:47–76, Mar 2003.

[10] D. Attwell and S. B. Laughlin. An energy budget for signaling in the grey matter of the brain. *J. Cereb. Blood Flow Metab.*, 21:1133–1145, Oct 2001.

[11] J. R. Lancaster. Simulation of the diffusion and reaction of endogenously produced nitric oxide. *Proc. Natl. Acad. Sci. U.S.A.*, 91:8137–8141, Aug 1994.

[12] T. C. Bellamy and J. Garthwaite. Sub-second kinetics of the nitric oxide receptor, soluble guanylyl cyclase, in intact cerebellar cells. *J. Biol. Chem.*, 276:4287–4292, Feb 2001.

[13] U. B. Kaupp. Family of cyclic nucleotide gated ion channels. *Curr. Opin. Neurobiol.*, 5:434–442, Aug 1995.

[14] T. M. Lincoln, N. Dey, and H. Sellak. Invited review: cGMP-dependent protein kinase signaling mechanisms in smooth muscle: from the regulation of tone to gene expression. *J. Appl. Physiol.*, 91:1421–1430, Sep 2001.

[15] M. Zonta, M. C. Angulo, S. Gobbo, B. Rosengarten, K. A. Hossmann, T. Pozzan, and G. Carmignoto. Neuron-to-astrocyte signaling is central to the dynamic control of brain microcirculation. *Nat. Neurosci.*, 6:43–50, Jan 2003.

[16] C. Krasel, J. P. Vilardaga, M. Bunemann, and M. J. Lohse. Kinetics of G-protein-coupled receptor signalling and desensitization. *Biochem. Soc. Trans.*, 32:1029–1031, Dec 2004.